Metallophilicity-Induced Clusterization: Single-Component White-Light Clusteroluminescence with Stimuli Responses

Xueqian Zhao,[1] Parvej Alam,[1] Jianyu Zhang,[1] Shiyun Lin,[4] Qian Peng,[5] Jun Zhang,[6] Guodong Liang,[7] Jing Zhang,[1] Herman H. Y. Sung,[1] Jacky W.Y. Lam,[1] Ian D. Williams,[1] Zheng Zhao,[3]* Xinggui Gu,[2]* Ben Zhong Tang[1,8,9,10]*

[1]Department of Chemistry, Hong Kong Branch of Chinese National Engineering Research Center for Tissue Restoration and Reconstruction, Institute of Molecular Functional Materials, Division of Life Science and State Key Laboratory of Molecular Neuroscience, The Hong Kong University of Science and Technology, Clear Water Bay, Kowloon, Hong Kong 999077, China.

[2]Beijing Advanced Innovation Center for Soft Matter Science and Engineering, College of Materials Science and Engineering, State Key Laboratory of Chemical Resource Engineering, Beijing University of Chemical Technology, North Third Ring Road 15, Chaoyang District, Beijing, 100029 China.

[3]School of Chemistry and Chemical Engineering, Southeast University, Nanjing, 211189 China.

[4]MOE Key Laboratory of Organic OptoElectronics and Molecular Engineering, Department of Chemistry, Tsinghua University, Beijing 100084, China.

[5]CAS Key Laboratory of Organic Solids, Institute of Chemistry, Beijing National Laboratory for Molecular Sciences, Chinese Academy of Sciences, Beijing 100190, China.

[6]School of Materials and Chemical Engineering, Anhui Jianzhu University, Hefei 230601, China.

[7]PCFM and GDHPPC Labs, School of Materials Science and Engineering, Sun Yat-sen University, Guangzhou, 510275 China.

[8]NSFC Center for Luminescence from Molecular Aggregates, SCUT-HKUST Joint Research Institute, State Key Laboratory of Luminescent Materials and Devices, South China University of Technology, Guangzhou 510640, China

[9]AIE Institute, Guangzhou Development District, Huangpu, Guangzhou 510530, China.
[10]HKUST-Shenzhen Research Institute, Shenzhen 518057, China.
Email: tangbenz@ust.hk

Abstract

The single-component white-light-emitting materials play an essential role in the next-generation solid-state lighting technology. Herein, linear gold(I) complex TPPGPA with conglobate trimer configuration trigged by aurophilic interactions in crystalline state was prepared to emit dual phosphorescent white-light emission, which also exhibited multi-stimuli responsive luminescent properties including thermochromism and mechanochromism. Specifically, the molecular packing mode and aurophilic interactions regulation were subtly taken as a functional relationship of the experimental correlation with emission. The results showed that the regulated aurophilic interactions and restriction of molecular motion were determined to be the precipitating factor and as a function of the wavelength and intensity, which is significant for the design guide about intelligent stimuli-responsive white-light emissive luminescent materials. Furthermore, their application in temperature-responsive white-light illumination was successfully demonstrated.

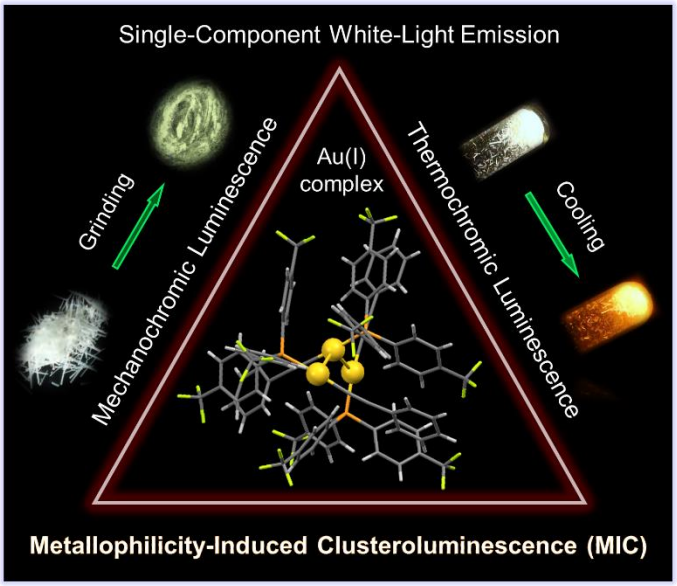

Introduction

White-light emission materials have attracted tremendous attention due to their high potential in displays and white-light illumination.[1] Compared with the complex hybrid system of different luminous components, single-component white-light emissive (SCWLE) materials are laudably admired for keeping the white color reproducibility and avoiding the notorious complicated device fabrications and energy transfer process.[2] To achieve SCWLE materials, the emission wavelength and intensity of the high energy (HE) band and low energy (LE) band need to be meticulously regulated and well balanced. Thus, panchromatic emission from a single molecule resulting in the generation of white light is limited observed.[3] After decades of tireless effort and development, some strategies are developed to realize the SMWLE, including π-excimers,[4] excited-state intramolecular proton transfer (ESIPT),[5] thermally activated delayed fluorescence (TADF),[6] aggregation-induced emission (AIE),[7] room temperature phosphorescence (RTP),[8] metal-metal interaction in metal-containing

complex[9] and so on.[10] For example, in 2009, Park et al.[11] have designed covalently linked two ESIPT moieties with the merit of anomalously large Stokes shift with less self-absorption to form frustrated energy transfer, thus generate pure white emission and further applied into OLED devices. Tang and his co-workers[12] also developed a pathbreaking strategy to achieve SMWLE by utilizing the nature of phosphorescence through heavy atom effect or anion-π^+ interaction to enhance the SOC to lead the efficient ISC process. The real model of the lampshade by 3D printing based on the RTP phosphor shows an extensive application prospect. In addition to the applications in displays and illuminations, if the ratiometric of multiple emission bands of SMWLE materials could be regulated by external stimulus, the application prospects could be significantly increased.[13] Tian and coworkers[14] utilized the self-folding behavior of the symmetric donor-acceptor-donor type structure to enhance charge transfer emissions to achieve SMWLE. The dual emissions could be finely regulated by various stimuli including solvent polarity, temperature, and host-guest interactions, which show potential application for thermometer or viscometer. What's more, according to Kasha's rule,[15] emissions are always inclined to decay form the lowest vibrational states resulting in monochromatic emission. Therefore, the nature of white light emission with multiple emission bands itself is fundamental interest and important, which deserves an in-depth study into the mechanism.

Some organic SMWLE materials have been designed and used as emitters for organic light-emitting diodes (OLEDs) to simplify the device fabrications, which has been discussed above. However, as only 25% of the singlets can be converted to the radiative emission in fluorescent organic molecules, their quantum yields are inevitably low. Hence, to improve the quantum yield intrinsically, phosphorescent transition metal complexes are chosen as common strategies. Both 25% of the singlet and 75% of the

triplet excited states can be harvested simultaneously.[16] Among them, gold-based complexes have a great potential to achieve extremely efficient luminescence and rich color for the rapid intersystem crossing process to the triplet state of the excited state.[17] For example, Credgington, and coworkers[18] introduce a linear donor-bridge-acceptor gold(I) light-emitting complexes, which enable solution-processed OLEDs with near-100% internal quantum efficiency at high brightness for the rapid and efficient utilization of triplet states. However, due to the easily formed aurophilic (gold···gold) interaction to achieve several accessible excited states, the photophysical property regulation and unravel the mystery of the aurophilicity through the rational design based on gold(I) complex is full of luxury and challenge.[19] The key issue is to resolve the functional relationship between luminescence and aurophilic interaction, which were unexpected since gold(I) centers have a [$5d^{10}$] closed-shell electronic configuration and should thus experience only weak van der Waals forces. However, this kind of interaction (7-12 kcal/mol) induced by relativistic effects endows gold force comparably even stronger than hydrogen bonds.[20] For all this, to take advantage of the gold(I)···gold(I) interaction to achieve the SCWLE is possible.[21] In 2013, Li and coworkers[22] developed a white-light emissive trinuclear gold(I) cluster with the CIE coordinates of (0.31, 0.33) both in the solution and solid-state. The monomer-excimer equilibrium gives rise to the white-light emission through the combination of the dual emission from the gold(I) monomer and the excimer induced by gold···gold interaction, which shows the designable potentials to regulate the aurophilic interaction to achieve white light emission. Even the aurophilicity has a significant influence on the emission peak and wavelength. Much attempts but a limited understanding of the factors that guide how aurophilicity influence the photophysical properties.[21a, 23] Precision control of molecular structure and stacking has been a vital approach to access the issue.

Whether there is an ideal prototype complex, which could be able to achieve precise regulation along with a keen insight into matters of aurophilicity, is unclear.

Herein, tris(para-(trifluoromethyl)phenyl)phosphine was taken as the coordinated ligand to incorporate the desired gold(I) complex, which on the other side combined with phenylethynyl group to form linear gold complex TPPGPA. In the crystalline state, complex TPPGPA was observed with compact packing of conglobate trimer state trigged by robust aurophilic interactions, that is metallophilicity-induced clusterization (MIC), with thermochromic dual phosphorescent white-light emission. Restriction of molecule motion and aurophilic interactions co-governed thermal equilibrium of ^{3}intracomplex (monomer) and ^{3}intercomplex (cluster) charge transfer was proposed to explain the distinct dual phosphorescence. With these distinctive cluster conformations and photophysical properties, we set out to determine changes in low energy emission as a function of gold…gold distance and look for a possible correlation between emission and aurophilic interactions to be a general rule. Finally, such white-light emissive crystals also perform well in polymer matrices, and their use in white-light illumination is further demonstrated by coating to blue light lamps.

Results and discussion

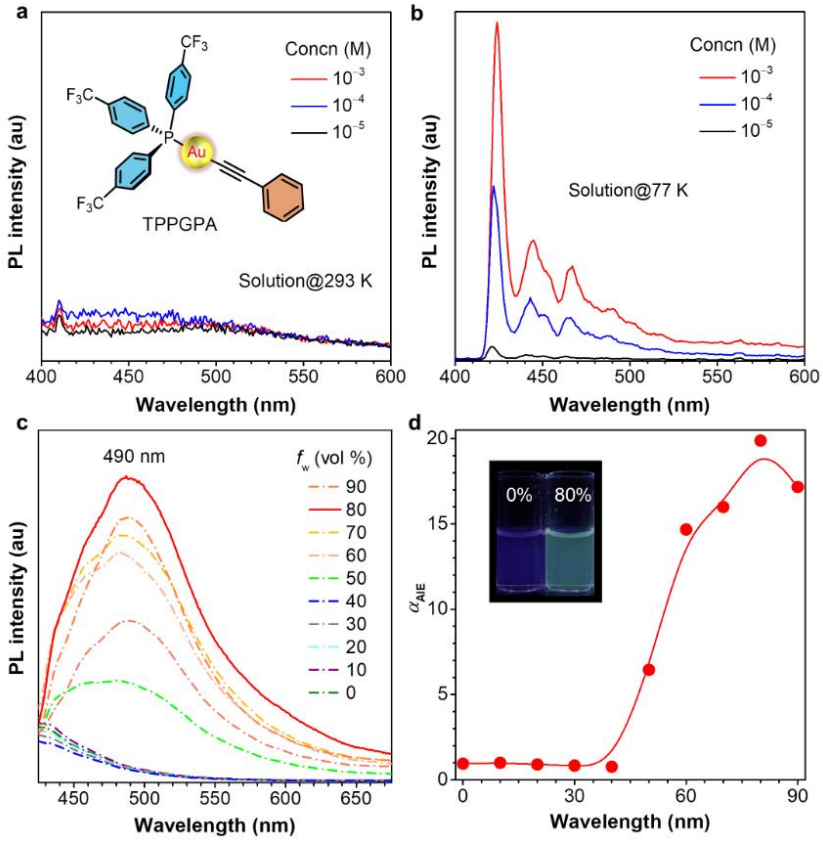

Figure 1. PL spectra of complex TPPGPA in dichloromethane solution with different concentrations taken at (**a**) 293 K and (**b**) 77 K. The inserts show the structure of TPPGPA and its electron cloud distributions in the gas state. (**c**) PL spectra of complex TPPGPA in DMF/water mixtures with different water fractions (f_w). (**d**) Plots of relative PL intensity (I/I_0) versus f_w. Concentration = 10^{-5} M; I_0 = intensity at f_w = 0%; The inserts show pictures taken under UV light. λ_{ex} = 360 nm.

The [tris(4-(trifluoromethyl)phenyl)phosphine]gold(I) phenylacetylide complex TPPGPA was synthesized[24] straightforwardly by reacting the equivalent amounts of phenylacetylene and chloro[tris(para-trifluoromethylphenyl)phosphine] gold(I) complex to afford a high yield of 75%. The complex was characterized by ^{1}H, ^{13}C, ^{19}F as well as ^{31}P nuclear magnetic resonance spectroscopy (Fig. S1-4), high-resolution mass spectrometry, elemental analysis to show analytical purity.

The optical properties of complex TPPGPA were first investigated using ultraviolet (UV) – visible (Vis) and photoluminescence (PL) spectra in the dichloromethane solution. Complex TPPGPA showed a sharp absorption peak at the range of 250 nm - 300 nm with an onset absorption peak at 311 nm, as shown in Fig. S5, which could be assigned to a ππ* transition of the complex. The emission in the dichloromethane solution with different concentration both in solution (293 K) and frozen states (77 K) was also checked. No or faint emission was detected even the concentration up to 10^{-3} M at room temperature while three narrow peaks at 423 nm, 443nm, and 464 nm appear in frozen forms at 77 K as depicted in Fig. 1a-b. These three peaks during 400 nm-500 nm should be the vibrational emissions of the TPPGPA monomer.[25] According to the restriction of intramolecular motion (RIM) mechanism, the non-emissive characteristic of complex TPPGPA in dilute solution should be possibly ascribed to its active intramolecular motion of flexible conformations. Thus, the AIE characteristic (Fig. 1c-d) was analyzed by studying its PL behaviors in dimethylformamide/water mixtures with different water fraction (f_w). At low f_w, very dim PL emission is observed while a new emission peak at around 490 nm appears in mixtures containing ca. 50–60% f_w. The PL intensity reaches its highest value when water fraction up to 80%. Despite this, the PL quantum yields still very low (QY < 1%). The observed emission could be ascribed to the phosphorescence nature from the monomer ^{3}ππ* state due to the large stocks shift. Loose aggregates and lack of efficient gold···gold interactions may be the leading cause of the low PL intensity in the aggregates.

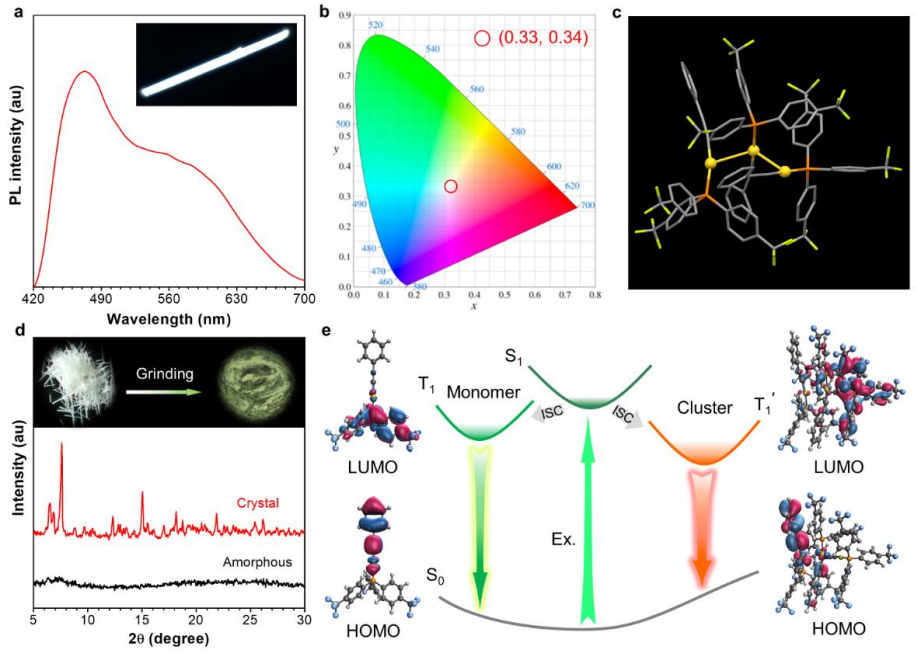

Figure 2. (**a**) PL spectra of crystalline TPPGPA, the inserts show the corresponding PL image, λ_{ex} = 360 nm. (**b**) CIE 1931 coordinates of crystalline TPPGPA. (**c**) The molecular structure of complex TPPGPA with thermal ellipsoids set at 50% probability. Hydrogen atoms are omitted for clarity. (**d**) Electron cloud distributions of the TPPGPA monomer (gas state) and trimer (solid-state) at ground state at the TD-DFT B3LYP/(6-31G**+LANL2DZ) level and the schematic illustration of emission from triplet state of the crystalline TPPGPA. (**e**) Powder XRD patterns of crystalline TPPGPA and its amorphous power, the inserts show the corresponding PL image.

Interestingly, crystalline TPPGPA features bright white-light emission at room temperature, which consists of dual emission bands centered at 475 nm and 578 nm, respectively, with a relatively high quantum yield of 15.5% and Commission Internationale de l'Éclairage 1931 coordinates of (0.33, 0.34) (Fig. 2a-b), which show the sporadic single component white-light emission in the crystalline state. To figure out the peculiar solid-state luminescent property, single-crystal XRD analysis was conducted as shown in Fig. 2c and S6. Crystal details were given in Table S1 in the

supporting information. The peculiar molecular packing motifs were noticed in the single crystals. The unit cell with a triclinic crystal system of trimers with relatively short Au-Au interactions falls in the range of 2.95 Å and 3.15 Å. These values are far below the sum of two Van der Waals' radii of gold (3.32 Å).[19a] Such a feature is strongly characteristic of so-called aurophilic interactions. The freedom of mutual rotation of the two complex axes to give staggering conformation to minimize molecular hindrance and free energy. The driving force of the intriguing assembly of trimers should come from the intrinsic intermolecular aurophilicity. Thus, we tentatively term the phenomenon as metallophilicity-induced clusterization (MIC). To figure out the relationship between the luminescence properties and their cluster arrangements in the solid state, controlling of the molecular arrangements of TPPGPA to tune their emission properties was comprehensively investigated. As shown in Fig. 2d, after grinding the crystalline TPPGPA, the white-light emissive crystals became greenish-yellow solid powers. Based on the PXRD results, the crystalline-to-amorphization phase transition is responsible for the mechanochromic behaviors. The PL spectra presented the detailed emission changes as depicted in Fig. S7. The short emission wavelength possessed a red-shift of 40 nm, while the long emission wavelength disappeared after grinding. Besides, the emission quantum yield decreased from 15.5% to less than 1%. Thus, we speculated that the long-wavelength emission was crystalline-dependent and induced by clusterization of the TPPGPA trimer.

To help better understand the origins of the dual-emission property, more experiments and DFT calculations were conducted. Firstly, emission lifetime of complex TPPGPA at various temperatures have also invastigated with monoexponential decay curves to confirm the phosphorescent nature of two excited states as shown in Fig. S8. Upon excitation at 360 nm, both of the two emission bands show microsecond scale lifetime. The average

lifetime of short-wavelength emission band and long-wavelength emission band increase from 6.9 μs to 9.5 μs and 10.8 μs to 17.6 μs, respectively, when lowering the temperature, which rules out the possibility of TADF mechanism. The excitation spectra measurements, as shown in Fig. S9, indicate that the two self-governed emission bands come from a similar excited state at 365 nm. The excitation-independent character could not only exclude the monomer-excimer dynamics but also indicate that the two emission bands come from the same excited state. Furthermore, TD-DFT calculations based on B3LYP/(6-31G**+LANL2DZ) was conducted. Frontier molecular orbitals for the single complex in gas state and trimer picked from the crystal structure are depicted in Fig. 2e. The highest occupied molecular orbital (HOMO) was distributed over the phenylethynyl group both in the monomer and the trimer cluster, while the lowest unoccupied molecular orbital (LUMO) was mainly located on the tris(para-(trifluoromethyl)phenyl)phosphine group. The difference is that these two kinds of charge transfer processes belong to monomer (introcomplex) charge transfer and cluster (intercomplex) charge transfer. Based on the above discussion, a rational mechanism was proposed, as shown in Fig. 2e. After excitation and relaxation to the S_1 state, fast intersystem crossing (ISC) happened to the high energy triplet state. This high energy state is assignable to the metal-perturbed $^3\pi\pi^*$ intracomplex charge transfer (CT). Meanwhile, the metallophilicity-induced clusterization of the trimer conformation endows the lower-lying triplet energy state (T′). The origin could tentatively assign as the intercomplex CT behavior. [26] This state is more sensitive to the aurophilic interaction, which offers an opportunity to achieve stimuli-responsive behavior by regulating the molecular packing mode and gold-gold interactions.

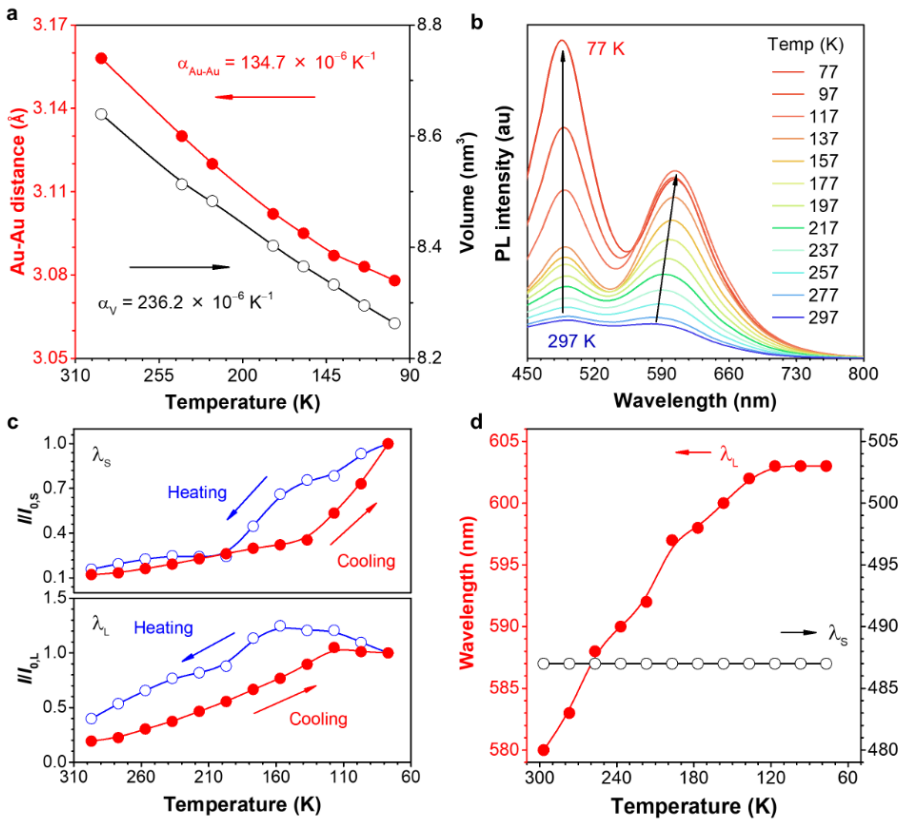

Figure 3. (**a**) Plots of unit cell volume (blue line) and Au-Au distances (red line) of complex TPPGPA crystals change at different temperatures. Inserts show the thermal expansion coefficient (α) of volume and Au-Au distances (average) of complex TPPGPA crystals. (**b**) PL spectra (cooling process), (**c**) comparable PL intensity of the cooling and heating process, and (**d**) plots of PL maximum wavelength of crystalline TPPGPA. $I_{0,S}$ = the intensity of the short-wavelength peak at 77 K, $I_{0,L}$ = the intensity of the long-wavelength peak at 77 K, λ_S = the short-wavelength emission band, λ_L = the long-wavelength emission band.

To precisely regulate the aurophilic interactions at the molecular level, we performed temperature variable single-crystal X-ray diffraction measurements over the range from 100 K to 293 K. Crystallographic details and refined values are given in Fig.3a and Table S1-S7, respectively. There was no evidence for the existence of structural phase transitions. However, the average coefficients of thermal expansion of *a*, *b* and *c* axial

were determined to be as large number of 53.3 × 10^{-6} K^{-1}, 121.5 × 10^{-6} $K^{-1,}$ and 72.1 × 10^{-6} K^{-1} during the temperature range studied companies by the coefficient of cubical expansion of 236.3 × 10^{-6} K^{-1}. The details are shown in Fig. S8 and S9. It is worth mentioning that the relative rate, α, at which a material expands with the increasing temperature usually falls within the range 0 × 10^{-6} K^{-1} to 20 × 10^{-6} K^{-1}. Herein, colossal positive thermal expansion in the crystal lattice was observed in this system, two order magnitude higher than that seen in other crystalline materials.[27] Besides, the thermal expansion coefficient of the average gold···gold distance located at the same magnitude (134.6 × 10^{-6} K^{-1}). Thus, we could speculate that the thermal expansion of lattice parameters was induced by the aurophilic interaction regulations in the crystal structure. The results show that the thermal stimulus could induce more subtle, but equally intriguing, systematic responses of aurophilic interactions in the crystal structure.

To verify the exact connection between photoluminescent property and aurophilic interactions, the temperature-variable PL spectra of crystalline TPPGPA during the range of 77 K – 297 K were systematically conducted as described in Fig. 3b. The PL intensities of both short and long wavelengths increase with the decrease of temperature. The long-wavelength emission peak redshift from 485 nm (293 K) to 603 nm (77 K) while the short-wavelength emission peak remains the same during the whole course. The definite trend of PL wavelength and intensity curve was drawn out in Fig. 3c-d. Specifically, the strength of the short-wavelength emission band gradually experienced a 9-fold increase with no shift during the whole journey with an inflection point in a steep rise at about 150 K, which could be the typical signal of the restriction of intramolecular motion (RIM) mechanism depicted in AIE community. After heating up, it can recover to its original state very quickly. On the contrary, the long-wavelength

emission intensity is difficult to recover in a short time when experiencing a cooling and heating cycle. The apparent hysteresis phenomenon indicates that the long-wavelength emission is packing-dependent. Temperature-variable Raman spectra was conducted as shown in Fig. S14. The asymmetric peak at 2122 cm^{-1} on behalf of the stretch of symmetric and anti-symmetric stretch vibrations of alkyne groups at room temperature. Large shifts and splitting of the main peaks with quite different slopes were observed with decreased temperature. Rigidification of the bond vibrations under low temperature is in charge of the peak splitting, which also confirmed the restriction of the intramolecular motion (RIM) mechanism.

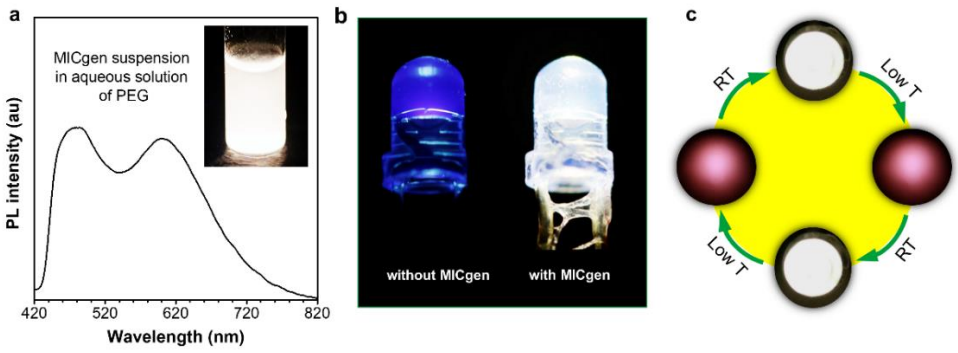

Figure 4. (**a**) PL spectra of white light emitters in poly(ethylene glycol) (PEG) solution. (**b**) Luminescent photographs of UV-LED lamps (emission wavelength: 360–370 nm) coated with PEG films without (left) and with (right) crystalline TPPGPA (side view). (**c**) Luminescent photographs (top view) of UV-LED lamps coated with PEG films with crystalline TPPGPA at different temperatures.

White light illumination was well performed in polymer matrices by crystalline TPPGPA. Firstly, Microcrystals were fabricated under ultrasound and uniformly dispersed in polyethylene glycol (PEG, *Mn* = 20 K) aqueous solution. The PL spectrum of the PEG solution with crystalline TPPGPA exhibited two emissions at 480 nm and 592 nm and the CIE coordinate was calculated to be (0.34, 0.35) (Fig. 4a), which

displays the excellent fatigue resistance white light emission. Then, we coated the PEG film loaded with complex TPPGPA onto UV-light-emitting diode (UVLED) lamps. Upon the excitation of 360 nm from this UV-LED lamp, the white light emission can be successfully realized, as demonstrated in Fig. 4b. Furthermore, the reversible thermochromic behavior of the PEG-coated lamp was further demonstrated in Fig. 4c based on the correlation between the emission and the temperature, which makes the materials based on TPPGPA as the potential use of the luminescence thermometers.

Summary

In summary, mononuclear gold(I) complex trimers were achieved by crystal engineers for white-light luminescent materials with CIE chromaticity coordinates of (0.33, 0.34) in the crystalline state. The distinct temperature-responsive behavior of short and long-wavelength emission bands supply an opportunity to look for a possible correlation between emission and aurophilic interactions. It was shown that aurophilic interactions and RIM mechanism co-govern the emission process. The complex structure and synthesis, though simple, could be as a model complex to reveal the relationship between structure and photophysical properties by two phosphorescent bands with distinct stimuli-response behaviors. Many phenomena, unsettled to date, will become more legible in the light of the correlation. At last, temperature-responsive white-light illumination in polymer matrices were well demonstrated.

Supporting Information

Supporting Information is available from the online website or from the author.

Acknowledgements

This project was financially supported by the National Natural Science Foundation of China (21788102), the Natural Science Foundation of Guangdong Province (2019B121205002 and 2019B030301003), the Research Grants Council of Hong Kong (16305618, 16305518, C6009-17G), the National Key Research and Development Prgram (2018YFE0190200), the Innovation and Technology Commission (ITC-CNERC14SC01), and the Science and Technology Plan of Shenzhen (JCYJ20180306174910791, and JCYJ20170818113530705 and JCYJ20170818113538482, and JCYJ20160229205601482). We thank for the experimental measurements.

Conflict of interest

The authors declare no conflict of interest

Keywords: white light emission • gold(I) complex • aurophilic interaction • stimuli-responsive materials• metallophilicity-induced clusterization (MIC)

Reference

[1] a) L. Zhang, X. L. Li, D. Luo, P. Xiao, W. Xiao, Y. Song, Q. Ang, B. Liu, *Materials* **2017**, 10; b) Z. Chen, C. L. Ho, L. Wang, W. Y. Wong, *Adv. Mater.* **2020**, 32, e1903269.

[2] a) Z. Xu, J. Gu, J. Huang, C. Lin, Y. Li, D. Yang, X. Qiao, A. Qin, Z. Zhao, B. Z. Tang, D. Ma, *Mater. Chem. Front.* **2019**, 3, 2652; b) M. S. Wang, G. C. Guo, *Chem. Commun.* **2016**, 52, 13194.

[3] J. Gierschner, S. K. Behera, S. Y. Park, *Angew. Chem. Int. Ed.* **2020**, DOI: 10.1002/anie.202009789.

[4] M. N. Yu Liu, Yue Wang, and Zhaomin Hou, *J. Am. Chem. Soc.* **2006**, 128, 5592.

[5] K. C. Tang, M. J. Chang, T. Y. Lin, H. A. Pan, T. C. Fang, K. Y. Chen, W. Y. Hung, Y. H. Hsu, P. T. Chou, *J. Am. Chem. Soc.* **2011**, 133, 17738.

[6] S. Gong, N. Sun, J. Luo, C. Zhong, D. Ma, J. Qin, C. Yang, *Adv. Funct. Mater.* **2014**, 24, 5710.

[7] Z. Xie, C. Chen, S. Xu, J. Li, Y. Zhang, S. Liu, J. Xu, Z. Chi, *Angew. Chem. Int. Ed.* **2015**, 54, 7181.

[8] Z. He, W. Zhao, J. W. Y. Lam, Q. Peng, H. Ma, G. Liang, Z. Shuai, B. Z. Tang, *Nature Commun.* **2017**, 8, 416.

[9] Y. T. Mingu Han, Zhao Yuan, Lei Zhu, Biwu Ma, *Angew. Chem. Int. Ed.* **2014**, 53, 10908.

[10] D. Li, J. Wang, X. Ma, *Adv. Opt. Mater.* **2018**, 6, 1800273.

[11] J. E. K. Sanghyuk Park, Se Hun Kim, Jangwon Seo, Kyeongwoon Chung, Sun-Young Park, Du-Jeon Jang, Begon˜a Milia´n Medina, Johannes Gierschner, Soo Young Park, *J. Am. Chem. Soc.* **2009**, 131, 14043.

[12] J. Wang, X. Gu, H. Ma, Q. Peng, X. Huang, X. Zheng, S. H. P. Sung, G. Shan, J. W. Y. Lam, Z. Shuai, B. Z. Tang, *Nat. Commun.* **2018**, 9, 2963.

[13] a) J. Miao, Y. Nie, Y. Li, C. Qin, Y. Ren, C. Xu, M. Yan, K. Liu, G. Liu, *J. Mater. Chem. C* **2019**, 7, 13454; b) Q. Wang, Q. Liu, X.-M. Du, B. Zhao, Y. Li, W.-J. Ruan, *J. Mater. Chem. C* **2020**, 8, 1433.

[14] D. Li, W. Hu, J. Wang, Q. Zhang, X. M. Cao, X. Ma, H. Tian, *Chem. Sci.* **2018**, 9, 5709.

[15] a) A. P. Demchenko, V. I. Tomin, P. T. Chou, *Chemical reviews* **2017**, 117, 13353; b) M. Kasha, *Discuss. Faraday Soc.* **1950**, 9, 14.
[16] V. W. Yam, V. K. Au, S. Y. Leung, *Chem. Rev.* **2015**, 115, 7589.
[17] a) M. C. Tang, A. K. Chan, M. Y. Chan, V. W. Yam, *Topics in current chemistry* **2016**, 374, 46; b) M. C. Tang, C. H. Lee, M. Ng, Y. C. Wong, M. Y. Chan, V. W. Yam, *Angew. Chem. Int. Ed.* **2018**, 57, 5463; c) A. Chu, F. K.-W. Hau, L.-Y. Yao, V. W.-W. Yam, *ACS Mater. Lett.* **2019**, 1, 277.
[18] A. S. R. Dawei Di, Le Yang, Johannes M. Richter, Jasmine P. H. Rivett, Saul Jones, Tudor H. Thomas, Mojtaba Abdi Jalebi, Richard H. Friend, Mikko Linnolahti, Manfred Bochmann, Dan Credgington, *Science* **2017**, 357, 159.
[19] a) H. Schmidbaur, A. Schier, *Chem. Soc. Rev.* **2012**, 41, 370; b) J. C. Lima, L. Rodriguez, *Chem. Soc. Rev.* **2011**, 40, 5442; c) H. Schmidbaur, A. Schier, *Chem. Soc. Rev.* **2008**, 37, 1931.
[20] a) A. L. Manuel Bardají, *J. Chem. Educ.* **1999**, 76, 201; b) q. P. D. W. B. Peter Schwerdtfeger, Anthony K. Burrell, Ward T. Robinson, and Michael J. Taylor, *Inorg. Chem.* **1990**, 29, 3593.
[21] a) R. N. McDougald, Jr., B. Chilukuri, H. Jia, M. R. Perez, H. Rabaa, X. Wang, V. N. Nesterov, T. R. Cundari, B. E. Gnade, M. A. Omary, *Inorg. Chem.* **2014**, 53, 7485; b) X. Y. Wang, Y. X. Hu, X. F. Yang, J. Yin, Z. Chen, S. H. Liu, *Org. Lett.* **2019**, 21, 9945.
[22] W. X. Ni, M. Li, J. Zheng, S. Z. Zhan, Y. M. Qiu, S. W. Ng, D. Li, *Angew. Chem. Int. Ed.* **2013**, 52, 13472.
[23] a) N. Glebko, T. M. Dau, A. S. Melnikov, E. V. Grachova, I. V. Solovyev, A. Belyaev, A. J. Karttunen, I. O. Koshevoy, *Chemistry* **2018**, 24, 3021; b) M. Jin, T. S. Chung, T. Seki, H. Ito, M. A. Garcia-Garibay, *J. Am. Chem. Soc.* **2017**, 139, 18115; c) M. M. Ghimire, V. N. Nesterov, M. A. Omary, *Inorg. Chem.* **2017**, 56, 12086; d) T. Seki, Y. Takamatsu, H. Ito, *J. Am. Chem. Soc.* **2016**, 138, 6252; e) C. Jobbágy, A. Deák, *Eur. J. Inorg. Chem.* **2014**, 2014, 4434.
[24] a) S. O. Keiko Nunokawa, Tsutomu Tatematsu, Mitsuhiro Ito, Jyun Sakai, *Inorg. Chim. Acta* **2001**, 322, 56; b) M. Jin, S. Yamamoto, T. Seki, H. Ito, M. A. Garcia-Garibay, *Angew. Chem. Int. Ed.* **2019**, DOI: 10.1002/anie.201909048.
[25] a) W. Lu, N. Zhu, C.-M. Che, *J. Organomet. Chem.* **2003**, 670, 11; b) W. L. Hsiu-Yi Chao, Yanqin Li, Michael C. W. Chan, Chi-Ming Che, Kung-Kai Cheung, and Nianyong Zhu, *J. Am. Chem. Soc.* **2002**, 124, 14696; c) W. Lu, W. M. Kwok, C. Ma, C. T. Chan, M. X. Zhu, C. M. Che, *J. Am. Chem. Soc.* **2011**, 133, 14120.
[26] a) Y. D. Zhennan Wu, Jiale Liu, Qiaofeng Yao, Tiankai Chen, Yitao Cao, Hao Zhang, and Jianping Xie, *Angew. Chem. Int. Ed.* **2019**, 58, 8139; b) K. Pyo, V. D. Thanthirige, K. Kwak, P. Pandurangan, G. Ramakrishna, D. Lee, *J. Am. Chem. Soc.* **2015**, 137, 8244.
[27] a) W. Cai, A. Katrusiak, *Nature Commun.* **2014**, 5, 4337; b) M. C. Andrew L. Goodwin, Michael J. Conterio, Martin T. Dove, John S. O. Evans, David A. Keen, Lars Peters, Matthew G. Tucker, *Science* **2008**, 319, 794.